

## LETTERS

# EphB receptor activity suppresses colorectal cancer progression

Eduard Batlle<sup>1,2,3</sup>, Julinor Bacani<sup>5</sup>, Harry Begthel<sup>1</sup>, Suzanne Jonkeer<sup>1,2</sup>, Alexander Gregorieff<sup>1</sup>, Maaïke van de Born<sup>1</sup>, Núria Malats<sup>6</sup>, Elena Sancho<sup>1,2</sup>, Elles Boon<sup>4</sup>, Tony Pawson<sup>5</sup>, Steven Gallinger<sup>5</sup>, Steven Pals<sup>4</sup> & Hans Clevers<sup>1</sup>

Most sporadic colorectal cancers are initiated by activating Wnt pathway mutations<sup>1</sup>, characterized by the stabilization of  $\beta$ -catenin and constitutive transcription by the  $\beta$ -catenin/Tcf4 complex<sup>2,3</sup>. EphB guidance receptors are Tcf4 target genes that control intestinal epithelial architecture through repulsive interactions with Ephrin-B ligands<sup>4,5</sup>. Here we show that, although Wnt signalling remains constitutively active, most human colorectal cancers lose expression of EphB at the adenoma–carcinoma transition. Loss of EphB expression strongly correlates with degree of malignancy. Furthermore, reduction of EphB activity accelerates tumorigenesis in the colon and rectum of *Apc*<sup>Min/+</sup> mice, and results in the formation of aggressive adenocarcinomas. Our data demonstrate that loss of EphB expression represents a critical step in colorectal cancer progression.

The genetic programme driven by  $\beta$ -catenin and Tcf-4 in colorectal cancer (CRC) closely resembles that of epithelial proliferative progenitors in the intestinal crypts<sup>3</sup>. As a case in point, EphB2 outlines epithelial cells in normal crypts, but is also expressed in the earliest neoplastic lesions caused by a mutationally activated Wnt pathway (Fig. 1a)<sup>4–6</sup>. Mutations in APC or  $\beta$ -catenin are present in the great majority of CRCs<sup>7–9</sup>. Consequently, constitutive  $\beta$ -catenin/Tcf-4 activity is present in virtually all CRC cell lines<sup>2,3</sup>. Unexpectedly, we found that *EPHB2* messenger RNA expression was greatly reduced in most CRC cell lines compared to our reference CRC cell line Ls174T (Fig. 1b). This finding was confirmed in a small panel of human CRC samples, including lymph node and liver metastases (examples within Fig. 1 and Supplementary Fig. 1). EphB2 could be observed in the progenitor cells at the bottom of crypts in adjacent normal tissue (Fig. 1d). All adenocarcinomas showed prominent nuclear  $\beta$ -catenin accumulation (Fig. 1c, e). Yet, nine out of ten showed extensive areas of highly reduced or completely absent EphB2 immunostaining (Fig. 1d, f). In metastases, colonizing CRC cells accumulated  $\beta$ -catenin, yet in five out of six cases EphB2 expression was absent or strongly diminished (Supplementary Fig. 1). We concluded that secondary silencing of EphB2 expression occurs frequently in malignant CRCs independently of  $\beta$ -catenin/Tcf-4 activity.

To determine at what stage of the adenoma–carcinoma progression EphB2 expression was lost in CRCs, we stained 30 dysplastic aberrant crypt foci (dACF), 31 small adenomas (diameter <5 mm), 12 large adenomas (diameter  $\geq$ 5 mm) and 36 carcinomas of different Dukes stages. The percentage of EphB2-positive cells was assessed and lesions were grouped. Group I lesions contained more than 80% EphB2-positive cells. Group II lesions contained 50–80% EphB2-positive cells. Group III lesions contained 20–50% positive cells,

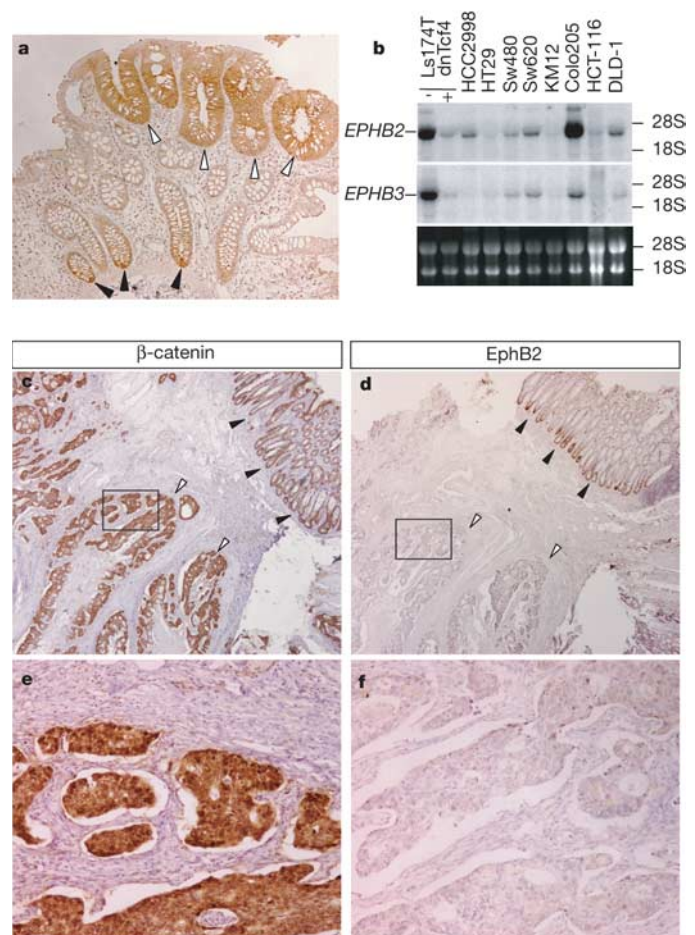


**Figure 1** | *EPHB2* is a  $\beta$ -catenin/Tcf-4 target gene but it is downregulated in advanced colorectal tumours and cell lines. **a**, EphB2 immunostaining of an early colorectal lesion from a Familial Adenomatous Polyposis patient. **b**, Analysis of *EPHB2* and *EPHB3* mRNA levels in a panel of CRC cell lines by northern blot. First two lanes correspond to Ls174T cells before (–) and after (+) expression of a dominant negative form of Tcf-4 (ref. 5). Bottom panel shows RNA loading. 28S and 18S indicate the migration of ribosomal subunits. **c–f**, Immunostaining using anti-EphB2 (**d, f**) or anti- $\beta$ -catenin antibodies (**c, e**) of an invasive colorectal adenocarcinoma. Panels **e** and **f** show high magnification pictures of the fields labelled with boxes in panels **c** and **d**. Black arrowheads point to EphB2-positive progenitor cells at the crypt base. White arrowheads point to tumour cells.

<sup>1</sup>Hubrecht Laboratory, Center for Biomedical Genetics, Uppsalalaan 8, 3584 CT Utrecht, The Netherlands. <sup>2</sup>Biomedical Research Institute, Barcelona Science Park, Josep Samitier 1-5, 08028 Barcelona, Spain. <sup>3</sup>Institució Catalana de Recerca i Estudis Avançats (ICREA), Passeig de Lluís Companys 23, 08010 Barcelona, Spain. <sup>4</sup>Department of Pathology, Academic Medical Center, 1105 AZ Amsterdam, The Netherlands. <sup>5</sup>Samuel Lunefeld Research Institute, Mount Sinai Hospital, 600 University Avenue, Toronto, Ontario, M5G 1X5, Canada. <sup>6</sup>Institut Municipal d'Investigació Mèdica, Dr Aiguader 80, 08003 Barcelona, Spain.

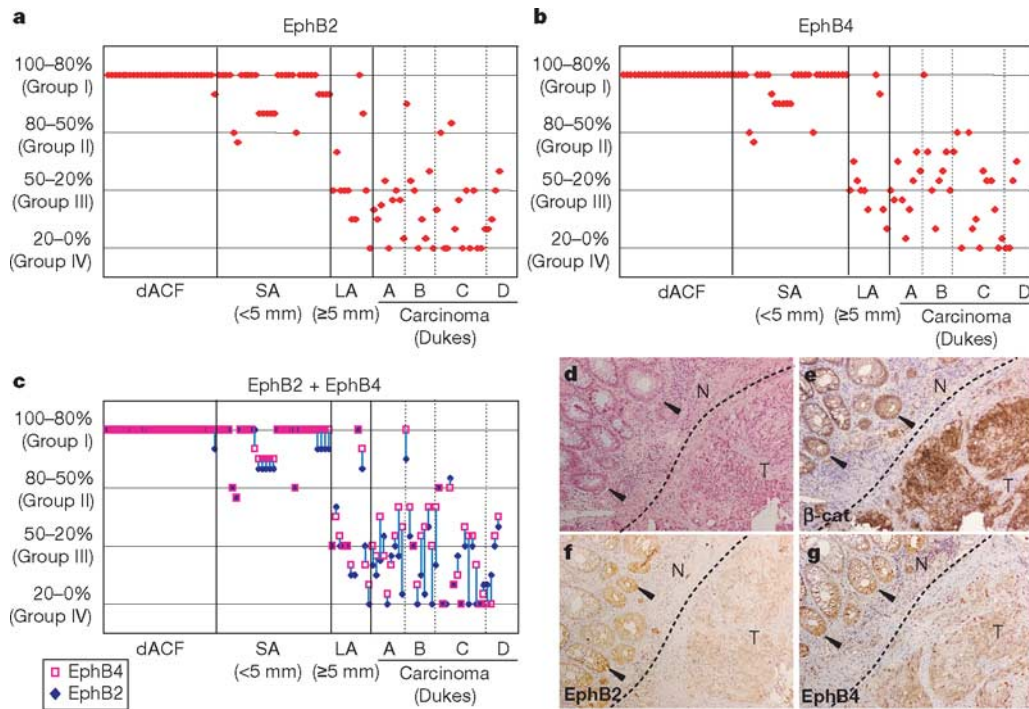


**Figure 2 | EphB2 and EphB4 are downregulated during CRC progression.** **a, b,** Classification of 108 colorectal lesions from patients according to the percentage of EphB2-positive (**a**) or EphB4-positive (**b**) cells and tumour stage. Each lesion is depicted as a red diamond. Dysplastic aberrant crypt foci (dACF), small adenomas (SA), large adenomas (LA) and carcinomas differed significantly between each other regarding EphB2 or EphB4 levels ( $P = 0.001$ ; Supplementary Figs 3 and 4). **c,** A strong overall correlation

( $r = 0.964$ ,  $P < 0.001$ ; Supplementary Fig. 5) was observed between the percentage of EphB2-positive (blue diamonds) and EphB4-positive (magenta squares) cells. A line links both scores in each lesion. **d-g,** Example of coordinated silencing of EphB2 (**f**) and EphB4 (**g**) in a carcinoma showing nuclear  $\beta$ -catenin accumulation (**e**). Dashed line depicts the boundary between tumour (T) and normal tissue (N). Arrowheads indicate staining in colonic crypts of healthy tissue.

whereas lesions showing less than 20% positive cells were classified in group IV. Staining in adjacent normal crypts was always used as an internal reference. Examples for each EphB2 group are shown in Supplementary Fig. 2. The mean score and stage for each lesion are depicted as a scatter plot in Fig. 2a. All (30 of 30) dACFs and 61% (19 of 31) of small adenomas retained EphB2 expression. Virtually all adenocarcinomas showed extensive loss of EphB2 expression (>50% of negative cells), while 25% of these malignant tumours were entirely EphB2-negative.

A strong association was found between histological tumour grade and EphB2 silencing independent of Dukes staging (Fig. 3a). Of 19 high grade adenocarcinomas, 14 completely lacked EphB2 expression and were classified in Group IV while the rest showed less than 50% EphB2-positive cells. The difference in EphB2 reactivity between high grade and low-intermediate grade adenocarcinomas had strong statistical significance ( $P = 0.017$ ; Mann-Whitney). In Group II/III, tumour masses were commonly composed of

intermingled EphB2-positive and -negative cells (Supplementary Fig. 2). However, some tumours contained areas that stained largely positive, adjacent to areas with downregulated EphB2 levels (Fig. 3a; cases linked by a dashed line). In these latter cases, the negative areas (Fig. 3f) were invariably high grade (Fig. 3e). *In situ* hybridization combined with immunohistochemistry on sequential sections demonstrated that in 12 out of 15 tumours analysed, *EPHB2* mRNA strictly followed protein expression (examples within Fig. 3b-g). The remaining three adenocarcinomas showed evident protein downregulation yet *EPHB2* mRNA remained present (Supplementary Fig. 6).

EphB3, the closest homologue of EphB2, was also silenced in CRC cell lines (Fig. 1b). Unfortunately, our antibodies did not allow consistent analysis of EphB3 expression in human tissue. However, by *in situ* hybridization on the above panel of 15 carcinomas, *EPHB3* mRNA was found to be downregulated with virtually identical patterns to that of *EPHB2* (Supplementary Fig. 7). Extending these

**Table 1 | CRC progression in *Apc*<sup>Min/+</sup> mice upon loss of *EphB3***

	<i>Ephb3</i> <sup>+/+</sup> ; <i>Apc</i> <sup>Min/+</sup>	<i>Ephb3</i> <sup>+/-</sup> ; <i>Apc</i> <sup>Min/+</sup>	<i>Ephb3</i> <sup>-/-</sup> ; <i>Apc</i> <sup>Min/+</sup>
Colorectal tumours* ( <i>n</i> = number of mice)	11 ± 6.15 ( <i>n</i> = 25)	15.67 ± 11.611 ( <i>n</i> = 55)	19.7 ± 12.9 ( <i>n</i> = 20)
Diameter ( <i>n</i> = number of tumours sized)	( <i>n</i> = 218)	( <i>n</i> = 306)	( <i>n</i> = 189)
<1 mm	48% (105)	42% (128)	44% (83)
1-5 mm	48% (104)	50% (153)	36% (69)
>5 mm†	4% (9)	8% (25)	20% (36)
Percentage of mice bearing invasive carcinomas‡	0% ( <i>n</i> = 19)	16% ( <i>n</i> = 37)	47% ( <i>n</i> = 17)

\* The mean number of colon polyps in the *Ephb3*<sup>-/-</sup>;*Apc*<sup>Min/+</sup> group is significantly different to that of the *Ephb3*<sup>+/+</sup>;*Apc*<sup>Min/+</sup> group ( $P = 0.015$ , *t*-test;  $P = 0.042$ , Mann-Whitney).  
 † The mean number of large (>5 mm) colorectal tumours in *Ephb3*<sup>-/-</sup>;*Apc*<sup>Min/+</sup> mice is significantly different to that of *Ephb3*<sup>+/+</sup>;*Apc*<sup>Min/+</sup> littermates ( $P = 0.004$ , *t*-test;  $P = 0.001$ , Mann-Whitney), and to that of heterozygous *Ephb3*<sup>+/-</sup>;*Apc*<sup>Min/+</sup> ( $P = 0.015$ , *t*-test;  $P = 0.006$ , Mann-Whitney). Yet, no significant differences were found regarding small (<1 mm) and medium size (1-5 mm) tumours between any of the groups. The three genotypes significantly differ regarding the number of large colorectal polyps ( $P = 0.002$ , Kruskal-Wallis test).  
 ‡ The complete loss of *Ephb3* is significantly correlated with the presence of invasion relative to *Ephb3*<sup>+/+</sup>;*Apc*<sup>Min/+</sup> ( $P = 0.001$ , Fisher's exact test) or to *Ephb3*<sup>+/-</sup>;*Apc*<sup>Min/+</sup> ( $P = 0.023$ , Fisher's exact test). The loss of one *Ephb3* allele was also sufficient to produce the invasive phenotype in six mice, but was not significantly correlated with invasion relative to wild-type littermates ( $P = 0.086$ , Fisher's exact test).

observations beyond our original array data<sup>5</sup> to all *EPHA* and *EPHB* genes, we found that *EPHB4* was also a Tcf target gene as its expression in CRC cell lines was inhibited upon blocking the Wnt cascade (Supplementary Fig. 8). Indeed, EphB4 was expressed in human colonic crypts and in early CRC lesions (Supplementary Fig. 9). Again its expression was lost in advanced colorectal tumours (Fig. 2b, Supplementary Fig. 9). Individual CRC samples showed similar percentages of EphB2- and EphB4-negative cells (Fig. 2c, Supplementary Fig. 5) and overlapping expression domains within each tumour (examples within Fig. 2d–g) implying that expression of these genes was silenced coordinately during CRC progression.

Although CRCs appear under strong selective pressure to down-regulate EphB2, EphB3 and EphB4, our observations did not prove a causal role for EphB silencing in tumour progression. To test this, we crossed the *Apc*<sup>Min</sup> allele into a transgenic mouse line that expresses in the intestinal epithelium a dominant-negative form of EphB2 lacking the cytoplasmic tail ( $\Delta^{\text{cy}}\text{EphB2}$ )<sup>4</sup>. The membrane anchored  $\Delta^{\text{cy}}\text{EphB2}$  molecule competes with EphB2, -B3 and -B4 receptors for binding of common Ephrin-B ligands, but is unable to transduce signals. Indeed,  $\Delta^{\text{cy}}\text{EphB2}$  transgenic mice phenocopy the individual intestinal phenotypes caused by disruption of *Ephb2* (defective cell positioning along the crypt-axis) and of *Ephb3* (loss of directional

sorting of Paneth cells)<sup>4</sup>, implying that the transgene faithfully mimics *Ephb* loss-of-function mutations. We never observed intestinal tumours in  $\Delta^{\text{cy}}\text{Ephb2}$  transgenics ( $n > 20$ ; ages  $> 6$  months).

*Apc*<sup>Min/+</sup> mice bear a truncated *Apc* allele<sup>10</sup> and develop dozens of adenomas in the small intestine<sup>11</sup> with accumulated nuclear  $\beta$ -catenin and high expression of EphB2 (ref. 4), EphB3 and EphB4 (Supplementary Fig. 8). Of note, unlike in humans carrying *Apc* mutations, macroscopic colorectal tumours in *Apc*<sup>Min/+</sup> mice are infrequent. Yet, multiple small dysplastic crypts, the earliest precursors of CRC, have been described in the colon of *Apc*<sup>Min/+</sup> mice<sup>12</sup>. We confirmed these observations. *Apc*<sup>Min/+</sup> mice showed only  $0.5 \pm 0.5$  macroscopic (diameter  $> 1$  mm) colorectal tumours, but developed multiple colonic microlesions ( $9 \pm 4$ ), the majority ( $> 85\%$ ) arising in the distal third of the large intestine ( $n = 5$  at 21 weeks of age).

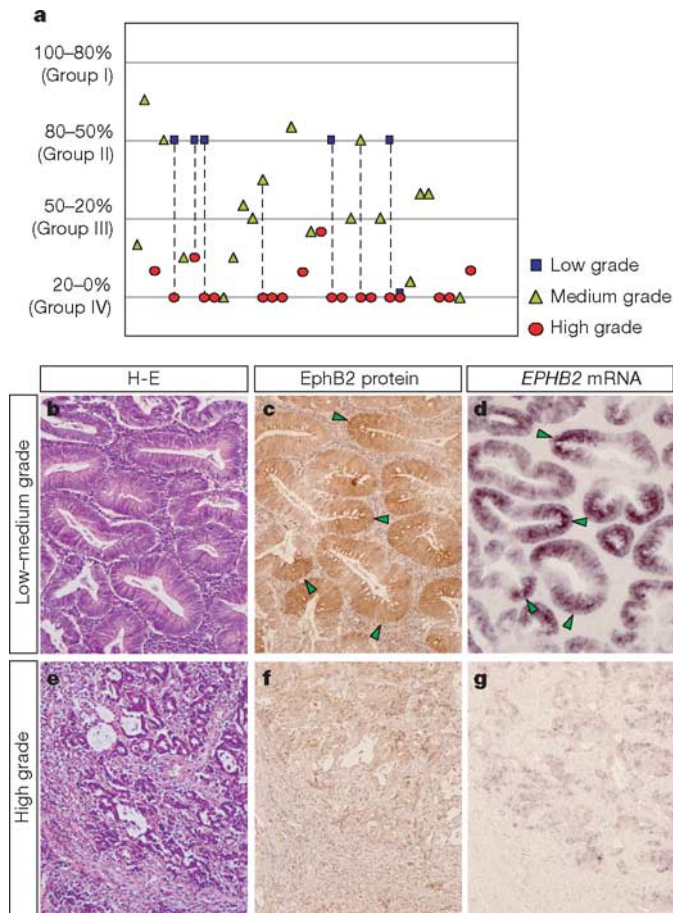


**Figure 3 | EphB2 downregulation correlates with higher histological tumour grade.** **a**, Correlation between the percentage of EphB2-positive cells and tumour grading in carcinomas. Areas of different grade within the same tumour are represented linked by a dashed line. **b–g**, Example of a single carcinoma showing a low-medium grade component (**b–d**) adjacent to a high-grade area (**e–g**). Consecutive sections were stained using anti-EphB2 antibodies (**c, f**) or by *in situ* hybridization with an *EPHB2* antisense cRNA probe (**d, g**). Arrowheads point to tumour glands that stained strongly positive for EphB2 protein and mRNA in the low-grade area. Panels **b** and **e** are haematoxylin–eosin (H–E) stainings.

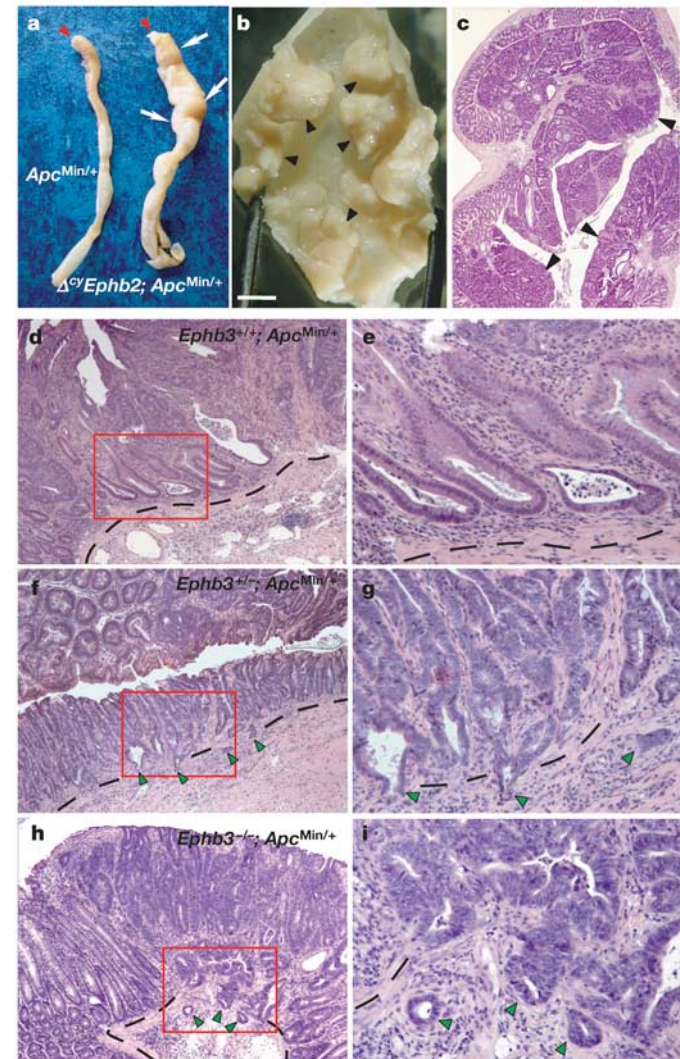


**Figure 4 | Accelerated colorectal tumorigenesis in *Apc*<sup>Min/+</sup> mice expressing  $\Delta^{\text{cy}}\text{EphB2}$  transgene or bearing *Ephb3*-null alleles.** **a**, Macroscopic comparison of the colon of *Apc*<sup>Min/+</sup> and  $\Delta^{\text{cy}}\text{Ephb2};\text{Apc}^{\text{Min}/+}$  mice at 21 weeks of age. Arrows point to distended areas in  $\Delta^{\text{cy}}\text{Ephb2};\text{Apc}^{\text{Min}/+}$  mice. Red arrowheads indicate the distal end. **b**, A dissected colorectum of a  $\Delta^{\text{cy}}\text{Ephb2};\text{Apc}^{\text{Min}/+}$  mouse showing multiple tumours (arrowheads). Scale bar, 5 mm. **c**, Colon histology in compound  $\Delta^{\text{cy}}\text{Ephb2};\text{Apc}^{\text{Min}/+}$  mice. **d–i**, Haematoxylin–eosin staining of representative colorectal tumours of *Ephb3*<sup>+/+</sup>;*Apc*<sup>Min/+</sup> (**d, e**), *Ephb3*<sup>+/+</sup>;*Apc*<sup>Min/+</sup> (**f, g**) and *Ephb3*<sup>-/-</sup>;*Apc*<sup>Min/+</sup> (**h, i**) mice. Dashed line depicts the muscularis mucosae. Green arrows point to invasive glands. Panels **e, g** and **i** show higher magnification pictures of the fields labelled with boxes in panels **d, f** and **h**, respectively.

Colonic microlesions in  $Apc^{Min/+}$  mice also accumulated high levels of  $\beta$ -catenin and expressed EphB2, EphB4 (Supplementary Fig. 10) and EphB3 (data not shown). Thus, although tumorigenesis is initiated frequently in the colorectum of  $Apc^{Min/+}$  animals, tumours do not progress beyond the earliest stage.

Compound  $\Delta^{cy}Ephb2;Apc^{Min/+}$  animals became moribund at the same age as control  $Apc^{Min/+}$  mice (~23 weeks). Post-mortem examination revealed decreased tumour counts in the small intestine of compound  $\Delta^{cy}Ephb2;Apc^{Min/+}$  ( $13 \pm 4$  macroscopic tumours per mouse compared to  $39 \pm 12$  tumours in control  $Apc^{Min/+}$  mice). Strikingly, all  $\Delta^{cy}Ephb2;Apc^{Min/+}$  mice analysed showed distension of the colorectum, unprecedented in  $Apc^{Min/+}$  mice (Fig. 4a). Dissection revealed  $11 \pm 3$  macroscopic tumours ( $n = 7$  at 21 weeks of age) clustered in the distal colon and rectum (Fig. 4b) compared with a single macroscopic tumour per mouse found in the distal colon of  $Apc^{Min/+}$  non-transgenic littermates ( $n = 2$ ).  $\Delta^{cy}Ephb2;Apc^{Min/+}$  colorectal tumours grew as large polypoid structures (mean diameter  $4.5 \pm 1.5$  mm). They were highly dysplastic with profound architectural and cytological distortion to a level that is highly uncommon in human or murine polyps but characteristic of carcinomas (Fig. 4c). In addition, we frequently observed pronounced cribriform tumour growth with areas of necrosis and prominent desmoplastic stromal reaction suggesting invasion of the lamina propria (Supplementary Fig. 11). Based on this, all  $\Delta^{cy}Ephb2;Apc^{Min/+}$  tumours were unequivocally classified as intramucosal adenocarcinomas (>30 tumours from 7 different mice), indicating a fully penetrant phenotype.

We also obtained  $Apc^{Min/+}$  mice carrying *Ephb3* null alleles (Table 1). Control  $Ephb3^{+/+};Apc^{Min/+}$  littermates developed significant numbers of colorectal polyps, presumably owing to the mixed genetic background or differences in mice stocks (see Methods section). Nevertheless, loss of EphB3 accelerated tumorigenesis.  $Ephb3^{+/-};Apc^{Min/+}$  and  $Ephb3^{-/-};Apc^{Min/+}$  mice consistently showed higher numbers and larger colorectal polyps than control littermates. 20% of the neoplasms in  $Ephb3^{-/-};Apc^{Min/+}$  were very large adenocarcinomas (diameter >5 mm) that rarely arose in  $Ephb3^{+/+};Apc^{Min/+}$  littermates. Furthermore, around half of the  $Ephb3^{-/-};Apc^{Min/+}$  animals developed carcinomas that invaded the muscle layer, a feature of malignancy that was not present in  $Ephb3^{+/+};Apc^{Min/+}$  tumours (Fig. 4d–i). Even a single *Ephb3* null allele enhanced invasive behaviour of  $Apc^{Min/+}$  tumours (Fig. 4f, g). Overall, these observations confirmed that reduction of EphB activity exacerbated colorectal tumorigenesis in  $Apc^{Min/+}$  mice and provided further evidence for a causal role of EphB silencing in CRC progression.

In the large intestine, dysplastic crypts and small polyps remain confined to small areas at the surface epithelium (Supplementary Fig. 10) where they are surrounded by normal cells expressing high levels of ephrin-B ligands (data not shown). Our observations indicate that EphB activity in CRC cells prevents further expansion and malignant progression of these benign lesions. We propose that human colorectal tumours overcome the restriction imposed by EphB receptors by silencing their expression. It has been recently reported that EphB2 becomes mutationally inactivated in a significant fraction of prostate tumours, thus reinforcing the idea that EphB activity acts as a tumour suppressor<sup>13</sup>. The mechanism behind the coordinated EphB downregulation in CRC is currently unknown. Our data indicate that silencing in CRC occurs at transcriptional or mRNA level, yet alterations only affecting protein levels are present in a subset of colorectal carcinomas.

We recently distinguished two different physiological functions for the  $\beta$ -catenin/Tcf-4 target gene programme in the intestinal epithelium: first, the maintenance of the undifferentiated, proliferative crypt phenotype, and second, the control of cell positioning along the crypt–villus axis through expression of EphB receptors<sup>4,5,14</sup>. The first function is maintained throughout all stages of carcinogenic progression<sup>5</sup>, presumably because it dictates an essential feature of

the transformed phenotype. During tumour progression, selection can occur against the expression of certain  $\beta$ -catenin/Tcf target genes, such as the *EPHB* genes. Our data illustrate the complexity of the mechanisms operating during tumour progression where initial mutational activation of a pathway confers certain selective advantages for tumour growth, but simultaneously imposes restrictions on immediate tumour progression. EphB2 has been proposed as a target for antibody-based cancer therapy on the basis of its relative overall upregulation in CRC compared to normal intestinal tissue<sup>15</sup>. This apparent discrepancy with our data might be explained by the fact that EphB2 expression in healthy intestine is restricted to less than 10% of all cells (that is, to a few progenitors at the crypt base). Thus, even carcinomas composed of only 25% EphB2-positive cells will show at least twofold higher overall EphB2 expression compared with normal tissue. Our current data warrant caution for therapeutic strategies, and underscore the necessity for careful, extensive validation of potential drug targets.

## METHODS

**Cell lines and northern blots.** Cell lines were obtained from the ATCC or the NCI. Cells were plated at low density ( $25,000$  cells  $cm^{-2}$ ) and cultured in RPMI 10% FCS for 24 h before harvesting. Ls174T cells expressing dominant negative Tcf4 upon addition of doxycycline were previously described<sup>6</sup>. Northern blot analysis of EphB2 was described elsewhere<sup>4</sup>.

**Antibodies and immunostaining.** The anti-EphB2-antibody was a goat affinity purified polyclonal directed against the extracellular domain (R & D Systems). We have previously characterized the specificity of this antibody<sup>4</sup>. Anti-EphB4 was a rabbit polyclonal generated against the 50 carboxy-terminal amino acids of the cytoplasmic tail (a gift from A. Ziemiecki, University of Bern)<sup>16</sup>. Anti- $\beta$ -catenin antibody was a mouse monoclonal generated against the C-terminal domain (Transduction Labs). Immunostaining methods are described in detail as Supplementary Information or elsewhere<sup>4,5</sup>.

**Sample collection and tumour scoring.** Paraffin-embedded tissues were obtained from the files of the Department of Pathology, Academic Medical Center, University of Amsterdam, The Netherlands. Adenomas were classified as small (diameter <5 mm) or large (diameter >5 mm). Colorectal carcinomas were staged according to the original Dukes classification; Dukes A, disease limited to the bowel wall; Dukes B, extensions through the deep muscle without metastases; and Dukes C/D, tumours with regional and/or distant metastases, respectively. Tumours were graded (high, medium and low) using standard histopathological criteria.

Each sample was classified by comparing the staining in the tumour with that of the bottom of the crypts in adjacent normal tissue. Tumour samples without normal tissue were not included in the study. Neither were samples of liver or lymph node metastases included, as they did not contain intestinal epithelial tissue as reference. Three independent observers (E.B., E.B. and S.P.) subjectively assessed the percentage of EphB2- or EphB4-positive cells within the tumour and classified them in one of the four groups detailed in the text. The final score is the mean of the classifications given by the three observers. In all lesions, standard deviation was always less than 1. Greater deviations corresponded to groups II and III while virtually all lesions completely positive or completely negative were given the same score by all observers. Tumour areas still showing perceptible EphB2 or EphB4 were evaluated as negative when intensity was severely reduced compared to the staining at the bottom of the crypts in adjacent normal tissue (that is, at least fourfold reduction).

**In situ hybridization.** *In situ* hybridization on formalin fixed-paraffin embedded pathological material was performed as previously described<sup>17</sup>. The protocol is described in detail in Supplementary Methods. DIG-labelled antisense complementary RNA probes corresponded to 3' end mRNA of human *EPHB2* (nucleotides 3682–4153; Human Gene Index THC2025076) or of human *EPHB3* (nucleotides 3530–4251; Human Gene Index THC2016077).

**Mice.** Transgenic mice expressing dominant negative EphB2 in the intestine under the control of the Villin-promoter were obtained by microinjection of single cell C57BL/6J  $\times$  CBA/J hybrid embryos as described previously<sup>4</sup>. Transgenic animals were crossed to the C57BL/6 strain for at least six generations before their mating with  $Apc^{Min/+}$  mice. The generation of *Ephb3*-null mice was previously described<sup>18</sup>. *Ephb3* mice were maintained in a mixed 129/sv:C57BL/6J (1:1) outbred background. All stocks of  $Apc^{Min/+}$  mice (Jackson Laboratory) were maintained in a homogenous inbred C57BL/6 background ( $N > 10$ ).

All experiments using  $\Delta^{cy}Ephb2$  mice were performed in the animal facility of Utrecht University, while *Ephb3* experiments were conducted in the facilities of Samuel Lunenfeld Research Institute. Different C57BL/6J; $Apc^{Min/+}$  mouse

stocks were used in both cases. Despite identical genetic background, we noticed that *Apc*<sup>Min/+</sup> mice housed in Samuel Lunenfeld Research Institute facility developed more colorectal polyps (on average, 5 macroscopic tumours per mouse at 5 months of age) than *Apc*<sup>Min/+</sup> housed in University of Utrecht facility (on average, 0.5 macroscopic tumours per mouse at 5 months of age). Both numbers are within the range of colorectal tumours reported previously for C57BL/6;*Apc*<sup>Min/+</sup> mice housed in these facilities<sup>19,20</sup> as well as in other laboratories<sup>11,12</sup> and probably reflect differences in the diet or husbandry conditions. All animal experiments were approved by the Animal Care and Use Committees of Utrecht University and of the Samuel Lunenfeld Research Institute.

**Tumour analysis in *Ephb3;Apc*<sup>Min/+</sup> mice.** At post-mortem examination, murine intestine was removed, opened along the longitudinal axis and fixed flat in 10% buffered formalin for 24 h at room temperature. Fixed intestines were stained with 0.5% methylene blue in distilled water for easier identification of small tumours, such as aberrant crypt foci (ACF). All colorectal lesions were identified under the dissection lens, counted and measured. Representative colon polyps were harvested, embedded in paraffin and sectioned at 5 µm. Histopathology was evaluated using standard techniques. True invasion through the muscle layer was determined by evaluating a minimum of three to six serial sections.

Received 9 February; accepted 11 April 2005.

1. Biens, M. & Clevers, H. Linking colorectal cancer to Wnt signaling. *Cell* **103**, 311–320 (2000).
2. Korinek, V. *et al.* Constitutive transcriptional activation by a beta-catenin-Tcf complex in APC<sup>-/-</sup> colon carcinoma. *Science* **275**, 1784–1787 (1997).
3. Morin, P. J. *et al.* Activation of beta-catenin-Tcf signaling in colon cancer by mutations in beta-catenin or APC. *Science* **275**, 1787–1790 (1997).
4. Batlle, E. *et al.* Beta-catenin and TCF mediate cell positioning in the intestinal epithelium by controlling the expression of EphB/ephrinB. *Cell* **111**, 251–263 (2002).
5. van de Wetering, M. *et al.* The β-catenin/TCF-4 complex imposes a crypt progenitor phenotype on colorectal cancer cells. *Cell* **111**, 241–250 (2002).
6. Kuhnert, F. *et al.* Essential requirement for Wnt signaling in proliferation of adult small intestine and colon revealed by adenoviral expression of Dickkopf-1. *Proc. Natl Acad. Sci. USA* **101**, 266–271 (2004).
7. Powell, S. M. *et al.* APC mutations occur early during colorectal tumorigenesis. *Nature* **359**, 235–237 (1992).
8. Sparks, A. B., Morin, P. J., Vogelstein, B. & Kinzler, K. W. Mutational analysis of the APC/beta-catenin/Tcf pathway in colorectal cancer. *Cancer Res.* **58**, 1130–1134 (1998).
9. Shitoh, K. *et al.* Frequent activation of the beta-catenin-Tcf signaling pathway in nonfamilial colorectal carcinomas with microsatellite instability. *Genes Chromosom. Cancer* **30**, 32–37 (2001).
10. Su, L. K. *et al.* Multiple intestinal neoplasia caused by a mutation in the murine homolog of the APC gene. *Science* **256**, 668–670 (1992).
11. Moser, A. R., Pitot, H. C. & Dove, W. F. A dominant mutation that predisposes to multiple intestinal neoplasia in the mouse. *Science* **247**, 322–324 (1990).
12. Yamada, Y. *et al.* Microadenomatous lesions involving loss of Apc heterozygosity in the colon of adult Apc(Min/+) mice. *Cancer Res.* **62**, 6367–6370 (2002).
13. Huusko, P. *et al.* Nonsense-mediated decay microarray analysis identifies mutations of *EPHB2* in human prostate cancer. *Nature Genet.* **36**, 979–983 (2004).
14. Sancho, E., Batlle, E. & Clevers, H. Live and let die in the intestinal epithelium. *Curr. Opin. Cell Biol.* **15**, 763–770 (2003).
15. Mao, W. *et al.* EphB2 as a therapeutic antibody drug target for the treatment of colorectal cancer. *Cancer Res.* **64**, 781–788 (2004).
16. Munarini, N. *et al.* Altered mammary epithelial development, pattern formation and involution in transgenic mice expressing the EphB4 receptor tyrosine kinase. *J. Cell Sci.* **115**, 25–37 (2002).
17. Gregorieff, A., Grosschedl, R. & Clevers, H. Hindgut defects and transformation of the gastro-intestinal tract in Tcf4(-/-)/Tcf1(-/-) embryos. *EMBO J.* **23**, 1825–1833 (2004).
18. Orioli, D., Henkemeyer, M., Lemke, G., Klein, R. & Pawson, T. Sek4 and Nuk receptors cooperate in guidance of commissural axons and in palate formation. *EMBO J.* **15**, 6035–6049 (1996).
19. Roose, J. *et al.* Synergy between tumour suppressor APC and the beta-catenin-Tcf4 target Tcf1. *Science* **285**, 1923–1926 (1999).
20. Lal, G. *et al.* Suppression of intestinal polyps in Msh2-deficient and non-Msh2-deficient multiple intestinal neoplasia mice by a specific cyclooxygenase-2 inhibitor and by a dual cyclooxygenase-1/2 inhibitor. *Cancer Res.* **61**, 6131–6136 (2001).

**Supplementary Information** is linked to the online version of the paper at [www.nature.com/nature](http://www.nature.com/nature).

**Acknowledgements** We thank A. Ziemiecki for EphB4 antiserum, and A. García de Herreros and C. Francí for help with mouse experiments.

**Author Information** Reprints and permissions information is available at [npg.nature.com/reprintsandpermissions](http://npg.nature.com/reprintsandpermissions). The authors declare no competing financial interests. Correspondence and requests for materials should be addressed to H.C. ([clevers@niob.knaw.nl](mailto:clevers@niob.knaw.nl)).